Collision-Free Infrared Multiphoton Dissociation of Silane

J. Makowe, O. V. Boyarkin, and T. R. Rizzo*

Laboratoire de Chimie Physique Moléculaire, École Polytechnique Fédérale de Lausanne, 1015 Lausanne, Switzerland

Received: July 19, 2000; In Final Form: September 27, 2000

We have measured an upper limit of 17 J/cm^2 for the threshold fluence for collision-free CO_2 laser IRMPD of silane by detecting the SiH_2 product in its electronic and vibrational ground state. The threshold drops to ~4 J/cm^2 when silane molecules are irradiated by all lines from a pulsed NH_3 laser. This value further drops to less than 2 J/cm^2 when the molecules are pre-excited to the first Si−H stretch overtone. Using the NH_3 laser on the 868 cm^{-1} line, the dissociation yield of pre-excited SiH_4 reaches saturation at a laser fluence of 6 J/cm^2. The substantial difference in the fluence threshold and optimal dissociation frequency of the ground and excited molecules allows us to perform highly selective dissociation of pre-excited silane in the presence of a large excess of ground-state molecules.

I. Introduction

Silane, SiH_4, is widely used in the semiconductor industry for deposition of silicon films, since it allows the production of SiH_x ($x = 0-3$) fragments in a well-controlled, chemically clean environment.[1] Dissociation of silane is thus a primary step in many silicon deposition processes, and a number of studies have been devoted to CO_2 laser infrared multiphoton dissociation (IRMPD) of this molecule.[2−8] These studies suggest that collisions, and hence relatively high pressures, are necessary for efficient multiphoton pumping of SiH_4 to the dissociation threshold. Despite the fact that it might be key for developing a laser driven molecular beam epitaxy technique, there is little known about collision-free IRMPD of silane.

Because silane has a relatively low density of vibrational states and sparse rotational structure, one expects dissociation via IRMPD to be difficult. In one early report,[3] no collision-free MPD of silane was observed using CO_2 laser pulses with fluence in excess of 150 J/cm^2. In another study,[8] IRMPD of silane at a pressure of 1 Torr was successfully achieved using 100 ns pulses from $^{12}CO_2$ and $^{13}CO_2$ lasers with energy fluence above 100 J/cm^2. It is well-known that to achieve efficient IRMPD of molecules, the frequency of the dissociating laser has to be shifted to the low-frequency side of the fundamental band of the pumped vibrational mode. Using a $^{13}CO_2$ laser, which emits frequencies to the red side of the Q-branch of ν_4, leads to a 10-fold increase in dissociation yield as compared to a $^{12}CO_2$ laser.[8] Unfortunately, the tuning range of the $^{13}CO_2$ laser is limited on the red side to about 880 cm^{-1}, and it is not clear if this is the optimum for the IRMPD process. We employ in the present work a simple, efficient, optically pumped NH_3 laser with a tuning range down to 780 cm^{-1}. Together with a conventional CO_2 laser, this source gives us the flexibility to investigate the dynamics of collision-free IRMPD in SiH_4.

The extremely high threshold fluence reported for IRMPD of silane has been attributed primarily to its low density of rovibrational states.[3,8] However, in these reports, dissociation of the molecule has been detected by monitoring the appearance of luminescence from electronically excited SiH_2,[7] SiH,[9] H_2, and H.[3] It is now established that the unimolecular reaction $SiH_4 \rightarrow SiH_2 + H_2$ is the lowest energy dissociation channel for SiH_4 in its electronic ground state, exhibiting a threshold of approximately 243 kJ/mol.[10] Moreover, there is evidence that this reaction has no barrier.[11] Thus, a silane molecule excited just above the dissociation threshold should have no energy available for fragmentation and/or electronic excitation of its dissociation products. The observed product excitation is likely to arise from high vibrational over-excitation of the parent SiH_4 molecules and/or secondary IR multiphoton excitation of SiH_x dissociation products by the intense CO_2 laser field. In either case, the appearance of the luminescence should require substantially higher fluence than the threshold value needed to dissociate silane. Using laser-induced fluorescence to monitor ground (electronic and vibrational) state SiH_2 products after collision-free IRMPD of SiH_4 may therefore give a lower value for the threshold fluence.

It is well-known that vibrational pre-excitation can greatly enhance IRMPD of polyatomics,[12] since it facilitates passing through the bottleneck region where the density of vibrational states is low. Moreover, the pre-excited molecules are closer to dissociation limit and need fewer photons, and hence lower fluence, to reach it. We have used this principle to develop a sensitive spectroscopic detection technique, called infrared laser assisted photofragment spectroscopy (IRLAPS), which we have applied to measure vibrational overtone spectra of polyatomic molecules cooled in a supersonic expansion.[13−18] In this technique, a CO_2 laser pulse selectively dissociates only molecules vibrationally pre-excited via a light-atom stretch overtone transition. The lower fluence and intensity thresholds for IRMPD of vibrationally pre-excited molecules as compared to ground-state molecules as well as different optimum dissociation frequencies provide a high degree of selectivity. Moreover, application of IRLAPS to measure overtone spectra of CH_3OH, CF_2HCl, and CF_3H has shown that the IRMPD detection step is not sensitive to details of the pre-excited state. In this case, the IRMPD photofragment action spectrum of the parent molecule directly reflects the overtone absorption spectrum. In addition to the practical importance of understanding the collision-free IRMPD dynamics of SiH_4, it is of interest

* To whom correspondence should be addressed.

10.1021/jp002566f CCC: $19.00
Published on Web 11/14/2000

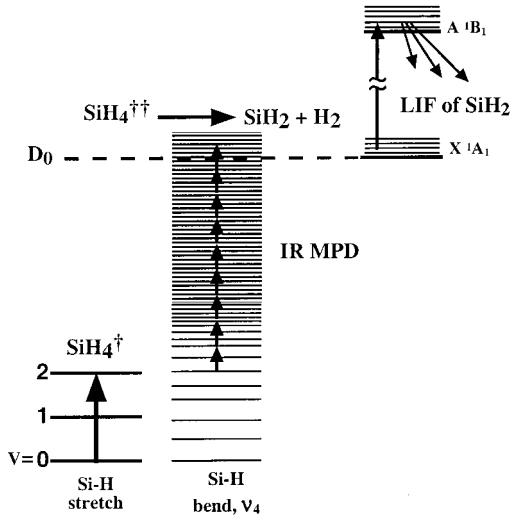

Figure 1. Schematic energy level diagram for IRMPD of vibrationally pre-excited silane.

to know whether a molecule this small (in terms of its density of states) is amenable to the IRLAPS technique for measuring high overtone spectra. To address this issue, we report here IRLAPS spectra of the first SiH stretch overtone level.

Silane is a spherical top molecule of T_d symmetry. The spectroscopy of its fundamentals and overtones has been extensively studied.[19−30] There are four fundamental vibrations: $\nu_1 = 2186.9$ cm^{-1} (A_1, Si−H symmetric stretch), $\nu_2 = 972.1$ cm^{-1} (E, Si−H symmetric bend, doubly degenerate), $\nu_3 = 2189.1$ cm^{-1} (F_2, Si−H asymmetric stretch, triply degenerate), and $\nu_4 = 913.3$ cm^{-1} (F_2, Si−H asymmetric bend, triply degenerate). Formally, only ν_3 and ν_4 are infrared active, although ν_2 also absorbs, borrowing a bit of oscillator strength from ν_4 through Coriolis coupling. Two distinct absorption bands, centered at 4309.4 and 4378.4 cm^{-1}, appear in the region of the first Si−H stretch overtone, assigned in local mode notation as transitions to the (2000, F_2) and (1100, F_2) states, although they are traditionally labeled using normal mode notation as $\nu_1 + \nu_3$ (F_2) and $2\nu_3$ (F_2), respectively.[24] A normal mode basis does not well represent the overtone states, since the $\nu_1 + \nu_3$ and $2\nu_3$ normal mode states are nearly degenerate and strongly coupled by a Darling−Dennison interaction. A local mode basis gives a more appropriate description of Si−H vibrational overtone levels, since it eliminates the strong anharmonic coupling, allowing them to be characterized by occupation numbers of the four local Si−H oscillators. The relationship between the local mode assignments and the traditional normal mode labels is based on the calculated correlation diagram, which indicates that the (2000, F_2) and (1100, F_2) states have as major components the zeroth-order $\nu_1 + \nu_3$ (F_2) and $2\nu_3$ (F_2) states, respectively.[31]

II. Experimental Section

Figure 1 shows a schematic energy level diagram for infrared multiphoton dissociation of vibrationally excited silane. An IR laser pulse excites the first vibrational overtone transition at ∼2.3 μm. A few nanoseconds later, a pulse from either a TEA CO_2 laser or an NH_3 laser promotes some fraction of the vibrationally excited molecules to energies above the dissociation limit via infrared multiphoton excitation. The SiH_2 fragments resulting from the unimolecular dissociation of SiH_4 are detected by a third laser via laser induced fluorescence (LIF). A vibrational overtone excitation spectrum is obtained by collecting the total SiH_2 fluorescence as a function of the frequency of the overtone excitation laser while keeping the frequencies of the dissociating and probe lasers fixed. In the experiments on IRMPD of ground-state SiH_4, the IR overtone excitation laser is switched off.

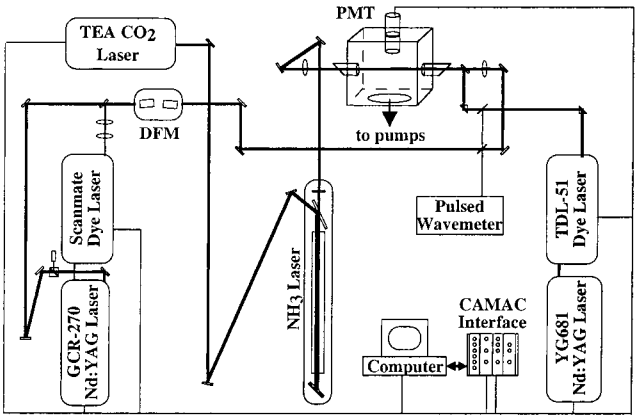

Figure 2. Experimental arrangement.

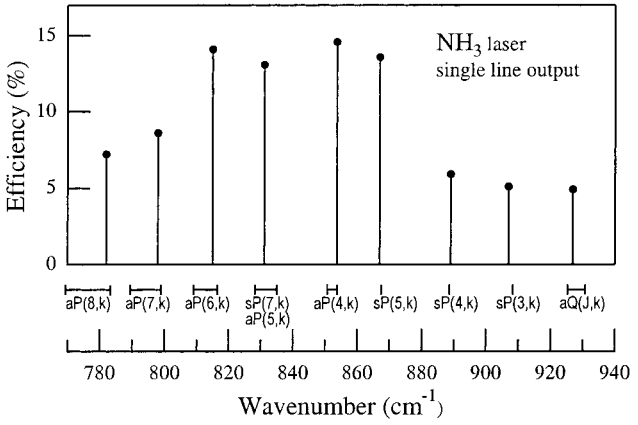

Figure 3. Tuning curve of the line-tunable NH_3 laser used for IRMPD.

The experimental apparatus we employ is shown in Figure 2. Infrared radiation at 2.3 μm for excitation of the first Si−H stretch overtone in SiH_4 is generated by difference frequency mixing the narrow-band (0.02 cm^{-1}) output of a Nd:YAG pumped dye laser (Spectra Physics GCR-250; Lambda Physik, Scanmate) with the single-mode fundamental of the same Nd:YAG laser in a $LiNbO_3$ crystal. Mixing 100 mJ of the Nd:YAG fundamental and 50 mJ of the dye laser (LDS-750) produces 3−5 mJ of the narrow-band infrared radiation. Absolute wavelength calibration is provided by a pulsed wavemeter (Burleigh WA-4500).

For a dissociating laser, we use either a line-tunable TEA CO_2 laser (Lumonics 841) or a home-built line-tunable NH_3 laser that is pumped by the CO_2 laser.[32] The tuning range of the CO_2 laser is limited on the low-frequency side to the 10P-(36) line (928.95 cm^{-1}) where it is capable of delivering ∼1.7 J/pulse, resulting in an estimated fluence of 30 J/cm^2 under our experimental conditions. The NH_3 laser expands the tunability range down to 780 cm^{-1}. Depending on the optical configuration of the resonator, the ammonia laser operates either in single-line or multi-line mode.[32] Figure 3 shows the typical output of the laser on the individual lines in single-line mode. In multi-line mode, 95% of the energy output occurs on lines below 870 cm^{-1}. This laser typically delivers 200−600 mJ/pulse, depending on the resonator configuration, the lasing line, and the CO_2 laser pump energy, and its low divergence enables us to reach fluences up to 30 J/cm^2 in the experiment. The time profile of

TABLE 1: IR MPD of Ground State SiH_4

line, cm^{-1}	effective fluence[a], J/cm^2	signal[b], a.u.
929[c]	17	252
800−870[d]	17	244
868	13	30
854	14	20
832	14	6
817	15	2
798	10	1
781	8	2

[a] Average fluence at full width half-maximum (fwhm) within the first millisecond of the laser pulse. [b] The signal is scaled to the same experimental conditions (sample pressure, PMT voltage) where necessary. [c] CO_2 laser 10P(36) line. [d] NH_3 laser in multiline configuration.

the CO_2 laser pulse consists of an intense, 270-ns wide peak (fwhm) containing 20% of the total energy, followed by a 3−4 μs long tail containing the remainder of the energy. The time profile of the NH_3 laser largely reflects that of the CO_2 laser but with a slightly smaller first peak.[32] The beam profile of the NH_3 and CO_2 lasers at the focus is measured by scanning a 50-μm slit and pyroelectric detector across the beam.

To probe the SiH_2 fragments at 553 nm [via the $\tilde{A}^1B_1$ (030) ← X $^1A_1$ (000) transition],[33] we use another Nd:YAG-pumped dye laser (Quantel YG681C, Quantel TDL 51) with R575 dye. A pulse energy of 2−3 mJ within the 0.15 cm^{-1} bandwidth from this laser is nearly enough to saturate the transition.

After being focused by a 60-cm CaF_2 lens, the overtone excitation laser beam is combined with the unfocused probe laser beam on a dichroic mirror, which directs them both through a Brewster angle CaF_2 window into the vacuum chamber. The dissociating laser is focused by a $F = 50$ cm ZnSe lens and introduced into the chamber on the opposite side through a Brewster angle NaCl window (Figure 2). The stainless steel vacuum chamber is pumped by a 6-in. diffusion pump to base pressure of 10^{-6} Torr. To avoid accumulation of dissociation products in the process of the experiment, the silane sample (Aldrich, semiconductor grade) slowly flows through the chamber at constant pressure in the range of 20−40 mTorr. The collision-free nature of the experiments has been carefully verified by measuring the pressure dependence of the LIF signal, which remains linear well above this pressure range.

An f/1, 50-mm focal length quartz lens collects the fluorescence of the SiH_2 fragments and images it onto a 3-mm slit in front of a photomultiplier tube (EMI 9635QB). The signal from the PMT is sent to a gated integrator (LeCroy, 2249SG) that integrates, digitizes, and transfers the signal to PC via a CAMAC interface. We run the CO_2 laser at 10 Hz repetition rate and both Nd:YAG lasers at 20 Hz, subtracting on alternate shots the background signal that arises mostly from scattered light of the probe laser. Each point in our spectra typically represents an average of 20−50 laser shots.

III. Results

A. IRMPD of Ground-State SiH_4. Table 1 summarizes the results of our study of collision-free IRMPD of vibrationally ground-state SiH_4, using the 10P(36) line of the CO_2 laser or the ammonia laser in both multi-line and single-line configurations. The SiH_2 dissociation fragments are detected by LIF at 1 μs after the beginning of the dissociating laser pulse. Because this part of the pulse contains only about half of the total energy, the "effective" fluence the molecules experience before we probe the fragment is correspondingly less than the total energy of a pulse. It is this "effective" fluence that is shown in Table 1 and reported in the text.

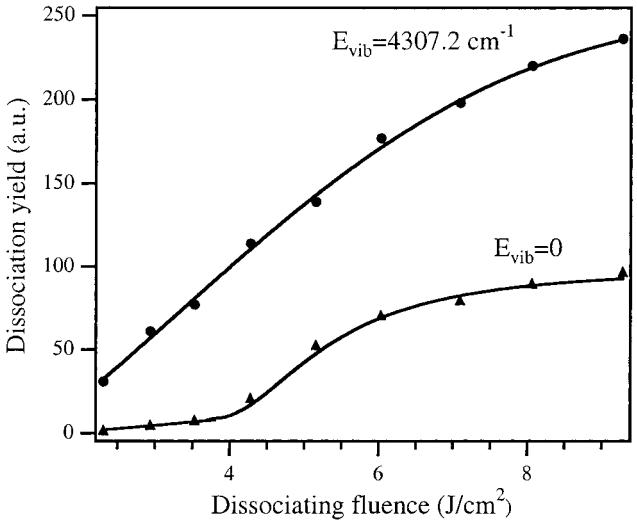

Figure 4. Dissociation yield of silane as a function of the fluence of multi-line NH_3 dissociating laser. The upper curve relates to SiH_4 molecules vibrationally pre-excited via the Q-branch of the $\nu_1 + \nu_3$ band. The lower curve relates to the ground-state molecules. The sample pressure is 30 mTorr.

The first important result in these measurements is that we observe collision-free CO_2 laser IRMPD of silane at a fluence of 17 J/cm^2, indicating that the threshold is significantly lower than that reported by Dzhidzhoev et al.[8] We believe that this difference arises largely from the different manner in which the two experiments detect dissociation. Laser induced fluorescence detection of ground-state SiH_2 radicals probes the dissociation of silane just above its lowest dissociation threshold, whereas detection of luminescence from electronically excited products may probe the threshold for a higher energy channel. The lower curve of Figure 4 shows the fluence dependence of the dissociation yield using the NH_3 laser in multi-line mode. One can see that the threshold fluence using this laser source is on the order of 4 J/cm^2, which is 25 times lower than that of Dzhidzhoev et al.[8]

The data of Table 1 also shows that if we use individual lines of our tunable NH_3 laser below 870 cm^{-1}, the dissociation yield drops by 1−2 orders of magnitude. The frequency dependence of the dissociation yield that we observe is consistent with that determined by Dzhidzhoev et al.,[8] where the maximum IRMPD efficiency is observed with a $^{13}CO_2$ laser 895 cm^{-1}.

B. IRMPD of Vibrationally Pre-Excited SiH_4. We now discuss the results of experiments in which up to a few percent of SiH_4 molecules are pre-excited by laser radiation at 2.3 μm to the first overtone of the SiH stretch vibration (see Figure 1). We first use the CO_2 laser tuned to 10P(36) line to dissociate the pre-excited molecules, and we monitor the fragment LIF signal as a function of frequency of the overtone excitation laser. Apart from a nonzero baseline, caused by IR MPD of the ground-state molecules, and a weak signal when the overtone laser is scanned across the $\nu_1 + \nu_3$ Q-branch, no detectable dissociation of the pre-excited molecules is observed in the region of the first SiH-stretch overtone level. This implies that with the CO_2 laser 10P(36) line we dissociate molecules from several rotational states but with a low dissociation yield. Only when the excitation laser is tuned to the Q-branch where these small contributions overlap do we detect a measurable signal. This situation changes dramatically when the NH_3 laser operating in multi-line configuration is employed as the dissociating laser. Figure 4 shows two plots of the SiH_2 LIF signal as a function of the dissociating laser fluence. The lower plot

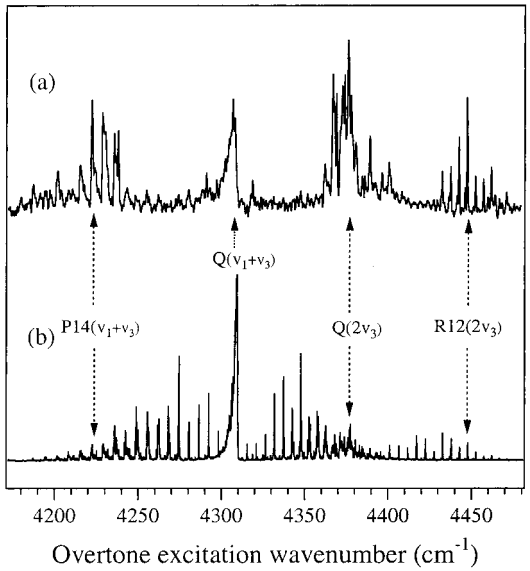

Figure 5. (a) Dissociation yield for vibrationally preexcited SiH_4 as a function of pre-excitation wavenumber. The NH_3 laser is used in multi-line configuration. (b) Photoacoustic spectrum of the first Si−H stretch overtone in SiH_4. The rotational assignment is taken from ref 20.

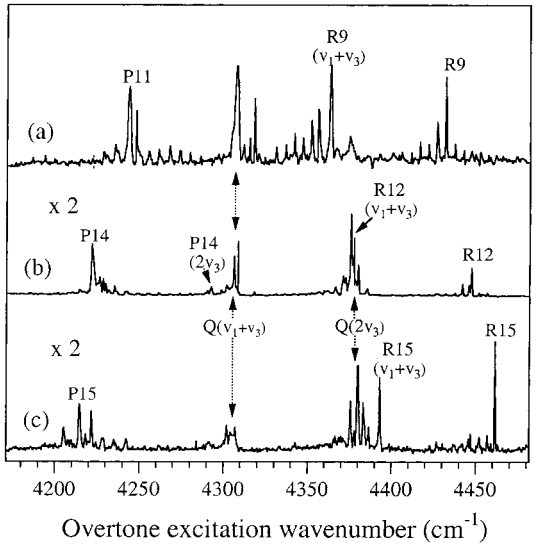

Figure 6. Dissociation yield for vibrationally pre-excited SiH_4 as a function of pre-excitation wavenumber with the dissociating laser is tuned to (a) 868 cm^{-1}, (b) 854 cm^{-1}, or (c) 832 cm^{-1}. Spectra b and c are magnified by a factor of 2 with respect to the spectrum a. The rotational assignment is taken from ref 20.

represents the dissociation of ground-state molecules in the absence of overtone pre-excitation. The upper plot shows the dissociation yield (with background signal from the dissociation of ground-state molecules subtracted) as a function of NH_3 laser fluence when we tune the overtone excitation laser to the $\nu_1 + \nu_3$ Q-branch. Despite the small fraction (∼2%) of pre-excited molecules, their contribution to the dissociation yield significantly exceeds that from the large fraction of SiH_4 molecules that do not undergo pre-excitation. The dissociation of pre-excited molecules exhibits monotonic growth with increasing fluence, suggesting that the threshold fluence is somewhere below the range investigated. We observed a similar lowering of the threshold fluence for dissociation upon vibrational pre-excitation in our work on CH_3OH[34] that we primarily attributed to two factors: (a) pre-excited molecules are already closer to the dissociation threshold and hence need 4−5 fewer photons to reach it; and (b) vibrational pre-excitation puts the molecule in a region of higher state density where bottleneck effects are greatly reduced.[34] This significant lowering of the threshold fluence can have important implications in laser isotope separation schemes insofar as it can alleviate the need for sharply focused laser beams.

The observed selectivity in dissociating vibrationally pre-excited SiH_4 molecules in the presence of a large excess of the ground-state molecules permits us to obtain an overtone excitation spectrum of SiH_4 using the IRLAPS scheme.[35,13] Figure 5a shows the relative dissociation yield of pre-excited silane as a function of the excitation wavenumber in the region of the first SiH-stretch overtone. Dissociation is achieved by the NH_3 laser operating in multi-line configuration, and the dissociation yield is measured by LIF detection of SiH_2. Figure 5b shows for comparison a photoacoustic spectrum of SiH_4 that reflects the absorption spectrum of the molecule in this region. It is clear that the dissociation spectrum is strongly distorted insofar as it differs from the absorption spectrum. Dissociation seems to be effective only for molecules pre-excited to rotational states with J quantum numbers in the range 9−15. Moreover, the dissociation yield is roughly the same for molecules pre-excited through the $\nu_1 + \nu_3$ combination band and the $2\nu_3$ overtone band, even though the intensity of the former (as illustrated in the photoacoustic spectrum) is about 4 times the latter. This implies that dissociation of molecules from the weaker $2\nu_3$ vibrational state is more efficient than dissociation from $\nu_1 + \nu_3$. We have performed the same experiment with the NH_3 laser operating on single strong lines (Figure 6a−c). Qualitatively the results are the same: dissociation is effective only when SiH_4 molecules are pre-excited to certain rotational states, and the dissociation yield is about the same for the two vibrational bands. With the NH_3 laser tuned to the 868 cm^{-1} line (Figure 6a), we observe the maximum dissociation efficiency at $J = 9$ and 10, and with the 854 cm^{-1} line (Figure 6b) the dissociation yield reaches a maximum for rotational states with $J = 13$. Dissociation with the 832 cm^{-1} line (Figure 6c) pushes the maximum to yet higher J (14 or 15).

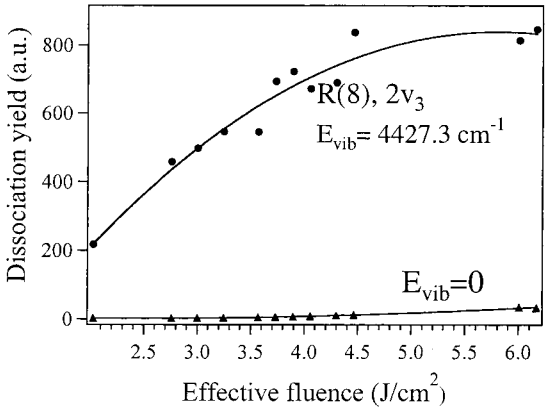

Figure 7. Dissociation yield as a function of energy fluence of the NH_3 dissociating laser at 868 cm^{-1}. The upper curve results from IRMPD of SiH_4 molecules vibrationally pre-excited to the $2v_3$ band via the R(9) transition. The lower curve represents IRMPD of ground-state silane molecules.

The 868 cm^{-1} line achieves the maximum dissociation yield of vibrationally pre-excited molecules, offering the best selectivity with respect to the dissociation of vibrationally ground-state molecules. Figure 7 shows the dissociation yield at this line as a function of the NH_3 laser fluence for ground-state molecules (lower curve) and for those pre-excited to $J = 10$ (upper curve) via the R(9) transition in the $2\nu_3$ band at 4432.4 cm^{-1}. The

dissociation yield appears to be saturated at an effective fluence of about 6 J/cm^2, suggesting that we dissociate almost all pre-excited molecules. At a fluence of about 3.5 J/cm^2, the dissociation signal from the pre-excited molecules is up to 230 times higher than that from the ground state molecules, which is almost completely suppressed. Taking into account that the overtone laser excites only about 10% of all molecules in the initial quantum state within the irradiated volume, this implies a dissociation selectivity for the pre-excited molecules of about 2300, assuming that for both ground state and pre-excited molecules the dissociation laser interacts with a single rotational state of approximately the same *J*, which is reasonable based upon the spectroscopy of the ν_4 fundamental.[21] This degree of selectivity results from the increase in the effective IRMPD cross section for the vibrationally pre-excited molecules at 868 cm^{-1}.

Our demonstrated ability to dissociate selectively vibrationally pre-excited molecules could potentially be employed in a process of two-color silicon laser isotope separation. If the first laser were tuned, for instance, to an isolated transition of the first Si−H stretch overtone in $^{29}SiH_4$, an IR pulse from a tunable ammonia laser could selectively dissociate the pre-selected isotopes. The selectivity we observe here would allow enrichment of the SiH_2 dissociation products in ^{29}Si from 4.67% natural abundance up to 99%.

IV. Discussion

It is clear from the data presented above that IRMPD of vibrationally pre-excited silane is considerably more efficient than that of ground state molecules, although this efficiency is strongly dependent upon the rotational state, the line of the ammonia laser employed, and the vibrational character of the pre-excited state. We present here a qualitative model to account for these features of the IRMPD dynamics.

A. Efficiency and Rotational Selectivity in IRMPD of Vibrationally Pre-Excited Silane. In SiH_4 excited to the first Si−H overtone, the density of vibrational levels (< 0.7/cm^{-1}) is, in general, still too low for IRMPD by a laser field of moderate fluence to be efficient. Our observation of high dissociation yield and low fluence threshold for IRMPD might therefore seem surprising at first. For vibrationally pre-excited molecules to be efficiently dissociated, the frequency of the dissociating laser should be in close resonance with rovibrational transitions from the excited state for at least the first few steps of infrared multiphoton excitation (IRMPE). In the excitation spectra of Figure 6a−c, the frequency of the ammonia laser used for dissociation is shifted to the low-frequency side of the ν_4 fundamental. This detuning compensates the anharmonic shift of the ν_4 frequency in the vibrationally excited molecules, allowing a resonance for the first step of IRMPE. When the density of rovibrational states is low, the same anharmonicity quickly tunes the transition out of resonance with the dissociating field upon further excitation steps, limiting the efficiency of IRMPD. However in the case of SiH_4, Coriolis splittings of the ν_4 transitions allows maintaining resonance. Each degenerate rovibrational transition in the ν_4 mode is split by Coriolis interaction to several components of slightly different frequencies. At each step of the multiphoton excitation process, different components of a transition to rovibrational states with the same *J* quantum number can tune into resonance with the dissociation field. For example, the P(10) transition of the ν_4 fundamental is split into eight components over a range of 10 cm^{-1}.[21] The number of components and the magnitudes of splittings increase with increasing *J*, and thus excitation to high rotational states enhances the probability for resonances in the multiphoton pumping process. The degree of splitting is even higher in a vibrationally pre-excited molecule, where Coriolis interaction is stronger, and thus higher orders of perturbation must be considered, further removing the degeneracy of rovibrational levels. Thus, Coriolis coupling is one important factor that permits efficient multiphoton excitation of vibrationally pre-excited SiH_4.

A second factor that increases the effective density of resonant states for muliphoton excitation of pre-excited SiH_4 as compared to unexcited silane molecules is the relaxation of symmetry restrictions in the former. The symmetry selection rules in silane allow transitions from the A_1 vibrational ground state only to vibrational states of F_2 symmetry. This means that vibrational overtone pre-excitation prepares a vibrational state of F_2 symmetry. However, the same selection rules allow vibrational transitions from the prepared state of F_2 symmetry to states of all other symmetry species of the T_d symmetry group: A_1, E, and F_2. Thus, the number of accessible rovibrational states for the first few steps of the multiphoton pumping process is greater after vibrational pre-excitation.

The mechanisms suggested above explain not only the high efficiency of IRMPD of SiH_4 molecules pre-excited to the first Si−H stretch overtone but also the observed rotational selectivity. Indeed, with a 10 cm^{-1} typical width for splittings of single *J* levels and 5−6 cm^{-1} spacing of rotational transitions in SiH_4, only molecules pre-excited to a maximum two adjacent rotational levels can be efficiently dissociated. Moreover, it is clear in this case that the frequency of the dissociating laser controls which *J* levels can be efficiently dissociated from the pre-excited state. As demonstrated in Figure 6, changing dissociating frequency by 36 cm^{-1} from 868 to 832 cm^{-1} changes the efficiently dissociated rotational state from $J = 10$ to $J = 16$, which are spaced by about the same value.

Not only is the dissociation process specific to a narrow range of rotational states, but the rotational state that has the optimum overlap with the dissociating ammonia laser lines is the same for the $2\nu_3$ and the $\nu_1 + \nu_3$ band. For this to be true, the anharmonic shift of the ν_4 mode used for multiphoton pumping must be close to the same for these two levels. There are two possible sources of anharmonic shift of the ν_4 frequency in a molecule vibrationally pre-excited to the first Si−H stretch overtone. One is the cross-anharmonicities with the ν_1 and ν_3 modes, x_{14} or x_{34}, and the other is the diagonal or intramode anharmonicity, x_{44}. The cross- anharmonic constants for SiH_4 are unknown, although they are likely to be small, since Si−H stretch vibrations are very good local modes and the calculated stretch−bend coupling constant is small.[24] This suggests that it is mainly the diagonal anharmonicity, x_{44}, that tunes ν_4 in the vibrationally pre-excited molecule in resonance with the dissociating frequency, although we cannot rule out the case in which the off-diagonal anharmonicities are significant but coincidentally equal. The results of double resonance spectroscopy of ν_4 suggest a value of 2.2 cm^{-1} for the x_{44} anharmonic constant,[36] which implies that on the order of two quanta in the ν_4 mode would be enough to bring the P(10) transition of the ν_4 band into resonance with the 868 cm^{-1} dissociating frequency allowing molecules pre-excited to $J = 10$ to be efficiently dissociated via IRMPE. This same dissociating frequency would be off-resonant for molecules pre-excited to other rotational states.

For the diagonal anharmonicity x_{44} to play the major role in tuning the ν_4 frequency into resonance with the dissociating lasers, the two local-mode zeroth-order states responsible for the absorption in the 4300 cm^{-1} region must contain some

percentage of other zeroth-order "dark" states mixed in that have a few quanta in ν_4. In general, there is no reason to expect that the coupling of $2\nu_3$ and $\nu_1 + \nu_3$ to such zeroth-order states should be the same. As described more fully below, we believe that it is precisely this difference of coupling strengths that gives rise to the difference in the relative intensities of the $2\nu_3$ and $\nu_1 + \nu_3$ bands between the photoacousting spectrum and the IRLAPS detected excitation spectrum.

B. Vibrational Selectivity in IRMPD of Vibrationally Pre-Excited Silane. The mechanism described above for the rotational selectivity of IRMPD from the pre-excited states of silane implies that there is a coupling between the $2\nu_3$ or $\nu_1 + \nu_3$ stretch states and the dark states containing quanta in the ν_4 bending vibration. Stretch−bend coupling in SiH_4 has been predicted theoretically to be weak.[24] This means that the states we observe in the spectrum contain mostly the character of the zeroth-order (2000, F_2) and (1100, F_2) stretch states with at most small amounts of ν_4 bending states mixed in. Nevertheless, the difference in even this weak coupling can give rise to the difference in intensites for the $2\nu_3$ and $\nu_1 + \nu_3$ bands observed in the IRLAPS spectrum. We can express the two vibrational eigenstates $\xi_{1,3}$ and $\xi_{3,3}$ related to the $\nu_1 + \nu_3$ and $2\nu_3$ levels as

$$\xi_{1,3} \approx a_1(2000) + a_2\varphi_4 \qquad (1)$$

$$\xi_{3,3} \approx b_1(1100) + b_2\varphi_4$$

where a_1, a_2, b_1, and b_2 are the expansion coefficients, (2000) and (1100) are the two zeroth-order local-mode states correlated with the $\nu_1 + \nu_3$ and $2\nu_3$ bands, respectively, and φ_4 is a zeroth-order state involving the ν_4 bending vibration. Because the coupling between stretches and bends is expected to be weak, it can be treated as a perturbation, implying that $|a_1|, |b_1| \gg |a_2|, |b_2|$ and

$$a_2 \approx \frac{W_{13}}{\delta_{13,4}}, b_2 \approx \frac{W_{33}}{\delta_{33,4}} \qquad (2)$$

where W_{13} and W_{33} are the coupling matrix elements between (2000) and φ_4 and (1100) and φ_4, respectively. The variables $\delta_{13,4}$ and $\delta_{33,4}$ represent the energy separation of φ_4 from the states (2000) and (1100), respectively. The intensities of overtone transitions to the eigenstates $\xi_{1,3}$ and $\xi_{3,3}$ in the IRLAPS spectrum are related to the coefficients as $I_{1,3} \propto (a_2)^2$ and $I_{3,3} \propto (b_2)^2$, since the spectrum is detected by monitoring the fragments from dissociation via IRMPD through the ν_4 vibration. Thus, relative intensity of what is mostly the $\nu_1 + \nu_3$ or $2\nu_3$ bands is determined by the ratio of the expansion coefficients of eq 2. If a bending dark state φ_4 is coupled more strongly to the (1100) than to the (2000) zeroth-order state ($W_{33} > W_{13}$) and/or it is closer to $\nu_1 + \nu_3$ band ($\delta_{33,4} < \delta_{13,4}$), then the dissociation yield will be higher when molecules are pre-excited through the $\nu_1 + \nu_3$ band, and the corresponding feature will appear more intense in the IRLAPS spectrum. While one could speculate as to the precise assignment of the φ_4 state(s) based on a simple counting of nearby low-order resonances, it is well-established that high order couplings and/or sequential couplings can be equally important in the absence of strong specific low order anharmonic couplings. In this case, even a qualitative analysis requires knowledge of the potential energy surface.[37,38]

V. Summary and Conclusions

We have measured an upper limit for the fluence threshold of collision-free CO_2 laser IRMPD of silane by detecting the SiH_2 product in its vibrational and electronic ground state. The detection of vibronically "cold" fragments suggests an IRMPD fluence threshold below 17 J/cm^2 when using the 10P(36) line of CO_2 laser, which is significantly lower than previous measurements.[8] When irradiated by all lines from a pulsed NH_3 laser, which emits 95% of its energy below 868 cm^{-1}, silane exhibits a threshold fluence for IRMPD of ~4 J/cm^2. This value drops to less than 2 J/cm^2 when the molecules are first pre-excited to the first Si−H stretch overtone.

Using the NH_3 laser on the 868 cm^{-1} line, the dissociation yield of pre-excited SiH_4 reaches saturation at a laser fluence of 6 J/cm^2. The low threshold and high efficiency in IRMPD of vibrationally pre-excited SiH_4 molecules as compared to ground state molecules results primarily from the higher density of rotational−vibrational states of proper symmetry and stronger couplings in the vibrationally excited molecules. Apart from the ordinary statistical increase upon vibrational excitation, there are two additional factors contributing to the increased density of states in the vibrationally pre-excited molecules. First, vibrational pre-excitation lifts symmetry restrictions on the selection rules, allowing more vibrational states to become accessible in IRMPD. Second, vibrational pre-excitation makes Coriolis couplings stronger, resulting in further finer splittings of rotational levels.

We have shown that efficient IRMPD of silane occurs only if the molecules are pre-excited to certain rotational states, which depend on the frequency of dissociating laser. We attribute this rotational selectivity to the relatively low density of vibrational states at this level of pre-excitation. Efficient dissociation requires the first few steps of IRMPE to be resonant. The vibrational pre-excitation shifts the frequency of the ν_4 mode to be in resonance with the dissociating frequency at a particular rotational level.

We also observe vibrational selectivity in IRMPD of pre-excited silane, insofar as the dissociation favors pre-excitation to the weak $2\nu_3$ band over the stronger (in absorption) $\nu_1 + \nu_3$ band. We suggest that this arises from stronger anharmonic coupling of the (1100, F_2) zeroth-order local-mode state to a dark state(s) containing bend excitation. Because of the rotational and vibrational selectivity in IRMPD of vibrationally preexcited SiH_4, the action spectrum detected via IRLAPS does not reflect a true absorption spectrum.

The substantial difference in the fluence thresholds and optimal dissociation frequencies of the ground state and excited molecules allows us to perform highly selective dissociation of pre-excited silane in the presence of a large excess of ground-state molecules. This vibrational energy selectivity of IRMPD can be as high as 2300 when the molecules are preexcited to the first Si−H stretch overtone, resulting primarily from an increase in IRMPD cross section upon vibrational pre-excitation.

Acknowledgment. We thank the École Polytechnique Fédérale de Lausanne and the Fonds National Suisse through Grant 20-52578 for support of this work.

References and Notes

(1) Kern, W.; Ban, V. S. Thin Film Processes; Vossen, J. L., Ed.; Academic: New York, 1978; p 257.

(2) Basov, N. G.; Markin, E. P.; Oraevskii, A. N.; Pankratov, A. V.; Skachov, A. N. *JETP Lett.* **1971**, *14*, 165.

(3) Deutsch, T. F. *J. Chem. Phys.* **1979**, *70*, 1187.

(4) Longeway, P. A.; Lampe, F. W. *J. Am. Chem. Soc.* **1981**, *103*, 6813.

(5) Jasinsky, J. M.; Estes, R. D. *Chem. Phys. Lett.* **1985**, *117*, 495.

(6) Borsella, E.; Fantoni, R. *Chem. Phys. Lett.* **1988**, *150*, 542.

(7) Borsella, E.; Caneve, L. *Appl. Phys. B* **1988**, *46*, 347.

(8) Dzhidzhoev, M. S.; Kamaev, S. V.; Popov, V. K.; Chugunov, A. V. *Sov. J. Quantum Elect.* **1990**, *20*, 441.
(9) Schmitt, J. P. M.; Gressier, P.; Krishnan, M.; de Rosny, G.; Perrin, J. *Chem. Phys.* **1984**, *84*, 281.
(10) Mick, H. J.; Roth, P.; Smirnov, V. N. *Kinet. Catal. Engl. Tr.* **1994**, *35*, 764.
(11) Viswanathan, R.; Thompson, D. L.; Raff, L. M. *J. Chem. Phys.* **1984**, *80*, 4230.
(12) Bagratashvili, V. N.; Letokhov, V. S.; Makarov, A. A.; Ryabov, E. A. *Multiple Photon Infrared Laser Photophysics and Photochemistry*; Harwood: Amsterdam, 1985.
(13) Boyarkin, O. V.; Settle, R. D. F.; Rizzo, T. R. *Ber. Bunsen-Ges. Phys. Chem.* **1995**, *99*, 504.
(14) Boyarkin, O. V.; Rizzo, T. R. *Proc. SPIE* **1995**, *2548*, 231.
(15) Boyarkin, O. V.; Rizzo, T. R. *J. Chem. Phys.* **1996**, *105*, 6285.
(16) Boyarkin, O. V.; Lubich, L.; Settle, R. D. F.; Perry, D. S.; Rizzo, T. R. *J. Chem. Phys.* **1997**, *107*, 8409.
(17) Boyarkin, O. V.; Perry, D. S.; Rizzo, T. R. *J. Chem. Phys.* **1999**, *110*, 11346.
(18) Boyarkin, O. V.; Perry, D. S.; Rizzo, T. R. *J. Chem. Phys.* **1999**, *110*, 11359.
(19) Wilkinson, G. R.; Wilson, M. K. *J. Chem. Phys.* **1966**, *44*, 3867.
(20) Brégier, R.; Lepage, P. *J. Mol. Spectrosc.* **1973**, *45*, 450.
(21) Johns, J. W. C.; Kreiner, W. A.; Susskind, J. *J. Mol. Spectrosc.* **1976**, *60*, 400.
(22) McKean, D. C.; Morrisson, A. R.; Kelly, M. I. *Chem. Phys. Lett.* **1984**, *109*, 347.
(23) Campargue, A.; Stoeckel, F.; Terrile, M. C. *Chem. Phys.* **1986**, *110*, 145.
(24) Chevalier, M.; De Martino, A. *J. Chem. Phys.* **1989**, *90*, 2077.
(25) Zhu, Q.-s.; Ma, H.; Zhang, B.; Ma, Y.; Qian, H. *Spectrochim. Acta* **1990**, *46A*, 1323.
(26) Zhu, Q.-s.; Zhang, B.; Ma, Y.; Qian, H. *Spectrochim. Acta* **1990**, *46A*, 1217.
(27) Zhu, Q.-s.; Qian, H.-b.; Ma, H. *Chem. Phys. Lett.* **1991**, *177*, 261.
(28) Zhu, Q.-s.; Campargue, A.; Stoeckel, F. *Spectrochim. Acta* **1994**, *50A*, 663.
(29) Coats, A. M.; McKean, D. C.; Steele, D. *J. Mol. Struct.* **1994**, *320*, 269.
(30) Sun, F. G.; Wang, X. G.; Zhu, Q. S.; Pierre, C.; Pierre, G. *Chem. Phys. Lett.* **1995**, *239*, 373.
(31) Halonen, L.; Child, M. S. *Mol. Phys.* **1982**, *46*, 239.
(32) Makowe, J.; Boyarkin, O. V.; Rizzo, T. R. *Rev. Sci. Inst.* **1998**, *69*, 4041.
(33) Inoue, G.; Suzuki, M. *Chem. Phys. Lett.* **1984**, *105*, 641.
(34) Boyarkin, O.; Rueda, D.; Rizzo, T.; Seyfang, G.; Quack, M. *J. Chem. Phys.* **2000**, to be published.
(35) Settle, R. D. F.; Rizzo, T. R. *J. Chem. Phys.* **1992**, *97*, 2823.
(36) Millot, G.; Hetzler, B.; Foy, B.; Steinfeld, J. I. *J. Chem. Phys.* **1988**, *88*, 6742.
(37) Pearman, R.; Gruebele, M. *J. Chem. Phys.* **1998**, *108*, 6561.
(38) Quack, M.; Willeke, M. *J. Chem. Phys.* **1999**, *110*, 11958.